Periodica Polytechnica
Mechanical Engineering

X-ray Analysis of Stents and Their Markers

59(1), pp. 30-34, 2015
DOI:10.3311/PPme.7748

Péter Nagy[1 *]

RESEARCH ARTICLE

Received 09 October 2014; accepted after revision 10 November 2014

Abstract

Balloon expandable stents can be used to treat coronary stenosis. During stent implantation, X-ray imaging is used. In order to assist the doctors, it was decided to improve the cardiovascular stents' X-ray absorption ability by placing a unique marker in the stent strut. Tantalum powder, with 98% purity and 3-10 μm grains diameter, was used as the stent integrated marker. The stents were laser cut from a 1.81 mm external diameter stainless steel tube. The integrated marker was made by laser ablation, micro-welding and cutting. The X-ray absorption ability of the stent struts with and without markers was compared and a new analyzing method was created by which the volume of the stent integrated marker can be determined. The stent integrated tantalum powder increased the stent's local X-ray visibility by 0.73%. A new index-number was introduced using which the stent's X- ray absorption ability can be estimated at the stent's planning stage.

Keywords

Marker volume, Nd:YAG laser micro-machining, stent marker, X-ray visibility

[1]Department of Materials Science and Engineering, Faculty of Mechanical Engineering, Budapest University of Technology and Economics, H-1521 Budapest, P. O. B. 91, Hungary

* Corresponding author, e-mail: npeter@eik.bme.hu

1 Introduction

Heart diseases are one of the leading causes of death in developed countries. One of the most common methods of treating coronary stricture is to use stents. The metal base material, coating and geometry of the stents can greatly vary [1,2]. In Europe at present the most commonly used stent base materials are austenitic stainless steel, cobalt chromium and platinum chromium alloys [2,3]. In order to improve the stent implantation procedure for doctors, markers are used to increase X-ray absorption. Its advantage is that it supports the precision of stent implantation, follow-up and identification [4,5].

At present, the tubes are manufactured by laser cutting. The methods of positioning the markers on them vary greatly. The markers are often made by braiding, crimping, knotting, extrusion, laser micro-welding or a mixture of any of these methods [5, 6]. Their shapes can vary; for instance, ring or disc. The markers' base material may be gold, platinum, silver, tantalum, niobium, tantalum, zirconium, hafnium [7-9].

In another study, it was shown that hole geometries of struts were suitable to store markers. These uniquely formed reservoirs were located on the stents' proximal and distal rings. The markers had a disc shape and they were fixed in the marker reservoirs by extrusion. Their base material may be both tantalum and gold [10].

Steegmüller R. and colleagues fixed tantalum, gold and platinum markers to nickel titanium stents by laser microwelding. They placed these in the reservoirs formed in the stent struts. Following laser welding, they conducted corrosion experiments where they found that a hole was formed on the platinum marker stent strut (a pitting-corrosion mark). They concluded that the X-ray absorption of both gold and platinum markers were excellent, however the markers damaged the base material's corrosive characteristics [11].

Scott H., in his patent, presented ring shaped markers that could be placed on the stent struts' proximal and distal ends by crimping. The markers' fixation could be performed by riveting in the borehole formed in/on stent struts. The base material of these may be platinum and tantalum [12].

Siekmeyer G. and colleagues, in their study, compared the characteristics of nickel titanium stents and markers. The markers that the comparison was based on were manufactured by riveting and micro-welding. The examined markers were made of gold and tantalum. The analysis was based on scanning electron microscopic images, results of mechanical voltage and corrosion examinations. The markers' fixation was graded by pressing the marker out from the reservoir and by comparing the forces needed to achieve this. The joints made by laser microwelding were removed from the marker reservoirs by using significantly greater compressive force, however, the technology's disadvantage was that it created seams. This uneven surface led to greater risks during implantation compared to the markers manufactured by riveting. Nonetheless, while manufacturing riveted markers, the risk of creating micro-cracks on the stent struts was greater [13].

Stinson S. J., in his patent, presented the manufacturing technology of metal matrix composite stents. He made the stents' tube base material using laser powder scattering technology. He made the metal matrix composite tube on a cylindrical substrate, which was removed from the inside of the tube by chemical etching, ignition or other mechanical ways at the end of the process. Then, the stent was formed from the tube by laser cutting. The base material of the component used as a marker maybe tantalum, niobium, gold, tungsten, hafnium, palladium or rhenium [14].

1.1 X-ray analysis

The ASTM F640 standard contains criteria regarding the X-ray visibility of medical implants and on how the implant should be separated from the background on an X-ray image. In Europe, currently, the MSZ EN ISO 25539-2:2013 standard is in use, which contains the elements of the previously withdrawn standard, however, it does not contain further refinements regarding to the stents' visibility (in comparison to the ASTM standard) [15-17].

Yunquiang et al., in their innovation, presented an image processing method by which images taken by imaging systems used in medical practice could be analyzed. Their algorithm, by the help of marker's placed on the stent, could estimate the relative positioning of the stent. Using this algorithm, the layered images taken by the computed tomography machine could be matched in such a way that it showed a clearer picture with more contrast. Hence, the stents were seen with higher contrast on the CT images. However, in the study, the authors did not give any numerical data regarding the X-ray visibility, and did not simulate the real surgical environment [18].

Thomas et al. took (X-ray) micro-computed tomography images after placing stents in artificial vessel segments. They modelled the vessel segment using a latex tube with 3 mm external diameter and 1 mm wall thickness, in which they placed an 8.6 mm long and 3.7 mm wide artificial occlusion. In their experiments, they used a 2.75 mm diameter wide and 13 mm long 316L austenitic stainless steel stent. They took micro-computed tomography images in axial and radial directions on stents expanded by 8, 12 and 17 bar pressure and on those that were not expanded. The images were taken with 5.3 μm resolution and 25 kV beam voltage. Their results were directed to the determination of the stents' expanding process and its efficiency against occlusion. They did not provide any numerical data regarding the X-ray visibility [19].

Colombo A. and colleagues summarized the main characteristics of the stents available in commercial use. They presented and ranked the stents and their markers combined with X-ray visibility. The authors categorized their findings into difficult, medium and good visibility groups. They did not provide numerical data assigned to the individual stents [20].

Ring G. analyzed the stents' X-ray visibility and worked out an objective index-number for the stents' X- ray visibility. Using an X-ray microscope (XiDAT XD6600 X-Ray Inspection system), 100 kV beam voltage and 1 W cathode heating parameters, he took images of the stent and its background. He defined the so-called visibility windows, their visibility graphs and using these, the relative visibility index (XRVREL (%)) parameter. The XRVREL parameter shows how big the visibility window's visibility graph integral (including the stent) is compared to the background's visibility graph integral [21].

2 Theory/calculation

In the past 10 years, the most commonly used marker materials have been tantalum, platinum and gold. Previously, markers were manufactured by braiding, crimping and extruding cladding, however, with the development of laser technologies, laser micro-welding fixing appeared. By laser melting, the so-called metal matrix stent can be made. One of its base material components is the marker material which provides X-ray absorption enhancement. Its advantage is that forming a separate marker storage unit (for instance, reservoirs) is not necessary.

In the literature, a method [21] that characterized the stents' X-ray visibility by quantitative and qualitative methods was found. There was no literature resource available to analyze and evaluate the X-ray visibility of stents' containing markers (especially the stents with markers made from multiple metals and by laser melting). Also, data on index-number, by which the stents' X-ray absorption ability could have been estimated in the planning phase, was not available.

The aim of this study was to develop a new type of stent by which the marker's direct contact to any type of vessel wall can be avoided. Markers integrated into stent struts were manufactured (tantalum powder with grain size 3-10 μm in diameter) using stent struts made of austenitic stainless steel tube with 1.81 mm external diameter and 0.10 mm wall thickness. Additionally, the aim was to develop a new method by which the quantitative relation between the marker and stent can be planned.

Knowing this, the stent's X-ray visibility could be characterized by numerical values already in the planning method.

3 Materials and methods

3.1 Laser micro-shaping and chemical etching

To make the markers integrated in the stent struts, a Lasag KLS 246 and a TRUMPF TruPulse 103 type pulsed mode Nd:YAG laser machines were used. The markers integrated in the stent struts were produced by laser ablation followed by chemical etching, laser micro- welding and cutting. The individual elements of the process are shown below:

The 1st element of the process

Laser ablation: The markers were placed in Sanocor Coronary Stent struts [22]. To store them, reservoirs were created by laser ablation. On the tube's surface, 1 mm long, 30-35 µm wide and 40-45 µm deep reservoirs were made using 20 µm diameter laser beam, 4.2 mJ energy, 0.02 ms impulse length, 2000 Hz pulse repetition rate, 5 mm/s speed and 10 bar oxygen gas pressure.

The 2nd element of the process

Chemical etching: From the reservoirs, burr formed during laser ablation was removed by using ultrasound cleaning equipment (Elmasonic S 70 H) and Avesta Pickling Bath 302 (HF, HNO3 diluted with half proportion of water) etchant. Through experimentation, the optimal parameters were determined. It was observed that using the room temperature etchant presented above, 180 seconds of treatment time was enough to remove burr from the reservoirs [23].

The 3rd element of the process

The marker's positioning and laser micro-welding: After filling up the reservoirs with tantalum powder, it was closed using laser welding technique. The optimal welding parameters were defined by experimentation. The average power and impulse length were changed in the available impulse mode laser welding machine. The energy was changed between 100 and 500 mJ and the welded joints were examined using a stereo microscope (Olympus SZX16) and the quality of the tantalum powder filled reservoirs was checked.

The 4th element of the process

Laser cutting: The laser cutting of stents was conducted using 20 µm diameter laser beams, 8.7 mJ energy, 4 bar pressure O_2gas, 4 mm/s cutting speed. These parameters were in compliance with those used by the Sanocor Stent manufacturer.

The 5th element of the process

Chemical etching: Following laser cutting, chemical etching was repeated to remove burr formed while cutting the stent. This process was performed in the same etchant used for the chemical etching of the reservoirs. Through experimentation, it was proved that 360 seconds of etching time in the etchant (at room temperature) was sufficient to completely remove the burr off the cut surface.

3.2 X-ray analysis

X-ray microscopic images of the tantalum marker stents integrated in the stent strut in their manufacturing stage using 1 W cathode heating and 100 kV beam voltage parameters (same parameters used in clinical practice) were taken. On the X-ray microscopic images, a sample each of a stent strut with the marker and without the marker and of the background were marked and their visibility windows were created (Fig. 1). The images in the visibility window (whose size and position can be arbitrarily chosen) were analyzed as an 8 bit grey toned image and the greyness histogram of the pixels in the window was determined. With the assistance of the greyness histograms, visibility graphs were generated based on the relation between the pixels level of greyness and X-ray absorption. The local relative X-ray visibility parameter (XRV_{LREL}) of the stent strut segments with and without markers was determined (correlated to background excluding a sample) and is presented in Table1.

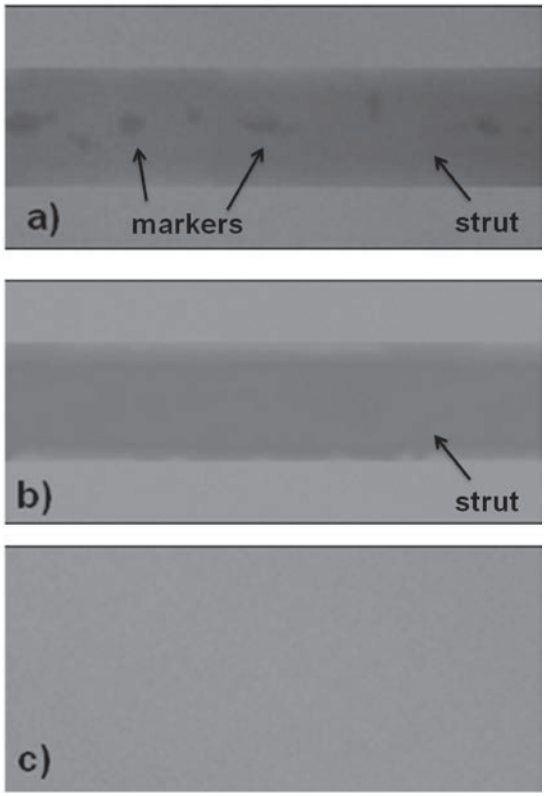

Fig. 1 a) Integrated stent marker b) stent strut without marker and c) the visibility window of a background without sample (1 W cathode heating, 100 kV beam voltage)

Table 1 Local relative visibility index of tantalum powder integrated in the stent strut

Comparison		XRV_{LREL} (%)
Empty background	Stent strut without marker	11.85
Empty background	Stent strut with marker	12.58

Tantalum powder integrated in the stent strut increased the stent strut's local X-ray visibility by 0.73%. As a result of this slight increase, the relation between the applied marker volume and the increase of the local X-ray visibility was determined. In view of this, the applied marker volume and the connected rate of the X-ray visibility can be planned. Following the X-ray analysis of the stent integrated markers, it was found important to determine through measurements the relation between the extent of X-ray absorption increase and the quantity of the applied base and marker materials. It was also necessary to study the effective marker volume by analyzing the X- ray microscopic images of the examined stent strut segment. The individual phases of the measuring methods are shown below:

- The determination of the applied tantalum marker's X-ray absorption ability in relation to material thickness (8 bit grey toned X-ray microscopic images, based on calibration level of greyness)
- The analysis of X-ray microscopic images of stents
- with integrated markers (Note: X-ray microscopic analysis parameters used during calibration)
- The identification of the marker territory seen on X- ray microscopic images
- The determination of the marker volume in the image (in the aspect of the known marker territory and local marker thickness)

A standard (etalon) was manufactured (note: from the same base material used for markers) to determine the material thickness. X-ray microscopic images were taken of the standard (using the same cathode heating and beam voltage parameters used for stents). Knowing the standard's exact geometrical dimensions (0.025 mm diameter tantalum wire), a calibration diagram was drawn up describing the relation between the pixels' level of greyness seen on the X-ray microscopic images and the material thickness assigned to them. Then, using an image analyzing software (JMicro Vision) the stent strut territory containing the marker was separated. Knowing the marker's territory and the material thickness belonging to the greyness levels, the volume of the stent integrated marker was calculated ($2.4x10^{-5}$ mm^3). The stent strut segments were compared with and without the marker and it was concluded that the 0.73% local X-ray visibility increase could be obtained by integrating a $2.4x10^{-5}$ mm^3 volume of tantalum powder marker.

As the next element of the measuring method, the volume of the examined stent strut segment (0.0073 mm^3) was determined. A unit of the stent integrated marker was marked and its volume ($6.2x10^{-6}$ mm^3) was determined. Here, it is important to note that the size of the marked marker area can be chosen arbitrarily. The stent strut was completely filled up lengthwise, increasing by 1-1 marker unit. With each marker unit increase, the stent strut's XRV_{LREL} parameter was determined. Knowing the measurement results, it can be pronounced that the examined (austenitic stainless steel) stent strut segment (0.0073 mm^3 volume) one unit stent integrated tantalum marker ($6.2x10^{-6}$ volume) filling increases the stent strut's XRV_{LREL} parameter value by 0.07%.

4 Results and Discussion

From 1.81 mm external diameter, 0.10 mm wall thickness austenitic stainless steel tube and from 3-10 μm grains diameter tantalum powder, a so-called stent with stent integrated marker can be manufactured using (pulsed Nd:YAG) laser equipment. On the stent strut's surface, a 1 mm long, 30-35 μm wide and 40-45 μm deep reservoir can be created using a 20 μm diameter laser beam, 4.2 mJ energy, 10 bar pressure oxygen gas and 5 mm/s centreline movement speed. After placing the tantalum powder in the reservoirs, these can be closed by laser micro-welding using a 400 μm diameter laser beam and 300 mJ energy in Argon shielding gas atmosphere. The stent integrated tantalum powder increased the stent strut's local X-ray visibility by 0.73%. Using our before described new measuring method, it was proved that this X-ray visibility increase can be obtained by integrating a 2.4x10-5 mm^3 volume tantalum powder marker. The examined (austenitic stainless steel) stent strut segment (0.0073 mm^3 volume) one unit stent integrated tantalum marker (6.2x10-6 volume) filling increased the stent strut's local relative X-ray visibility parameter value by 0.07%.

5 Conclusion

Using laser micro-welding, a so-called stent integrated marker can be created which increases the stent's X-ray visibility. Our before described new measuring method was worked out by the analysis of X-ray microscopic images, by which the stent integrated marker's quantity can be determined. The X-ray visibility of a stent with and without marker was compared. It was able to determine what quantity of marker can acquire how much increase in X-ray visibility. The further aims are to produce a large number of stents with integrated markers for more investigations and also to use this measurement method for a large number of stent types.

Acknowledgement

This work is connected to the scientific program of the 'Development of quality-oriented and harmonized R+D+I strategy and functional model at BME' project. This project is supported by the New Hungary Development Plan (Project ID: TÁMOP-4.2.1/B-09/1/KMR-2010-0002). The work reported in the paper has been developed in the framework of the project, 'Talent care and cultivation in the scientific workshops of BME' project. This project is supported by the grant TÁMOP-4.2.2.B-10/1-2010-0009.

The author thanks Judit Türk for English proof-reading.

References

[1] Bognár, E., Ring, G., Balázs, T., Dobránszky, J. "Investigation of Drug Eluting Stents." *Material Science Forum.* 589. pp. 361-366. 2008. DOI: 10.4028/www.scientific.net/msf.589.361

[2] Talha, M., Behera, C. K., Sinha, O. P. "A review on nickel-free nitrogen containing austenitic stainless steels for biomedical applications." *Material Science and Engineering C.* 33 (7). pp. 3563-3575. 2013. DOI: 10.1016/j.msec.2013.06.002

[3] Grogan, J. A., Leen, S. B., McHugh, P. E. "Comparing coronary stent material performance on a common geometric platform through simulated bench testing." *Journal of the Mechanical Behaviour of Biomedical Materials.* 12. pp. 129-138. 2012. DOI: 10.1016/j.jmbbm.2012.02.013

[4] Kertész, A., Bognár, E., Micsik, T., Dévényi, L. "Stent fracture analysis." *Material Science Forum.* 729. pp. 391-396. 2013. DOI: 10.4028/www.scientific.net/MSF.729.391

[5] Kutryk, M. J. B., Serruys, P. W. "*Handbook of coronary Stents.*" 3rd edition. London, Martin Dunitz. 2000.

[6] Paszenda, Z. "Use of coronary stents material and biophysical conditions." *Journal of Achievements in Materials and Manufacturing Engineering*. 43(1). pp. 125-35. 2010.

[7] Lam, S. S., Frantzen, J. J., Khosravi, F. "*Radiopaque stent markers.*" US patent 5725572. Advanced Cardiovascular System. 1998.

[8] Jonathan, S. S., Claude, O. C. "*Radiopaque markers and method of using the same.*" US patent 6340367. Boston Scientific Scimed Inc. 2002.

[9] Fulkerson, J. D., Bales, T. O., Jahrmarkt, S. L. "*Vascular stent with radiopaque markers.*" US2004/0015229. Syntheon. 2004.

[10] Pinchasik, G., Ramat, H. "*X-ray visible stent.*" EP0709068. Medinol Ltd. 1996.

[11] Steegmüller, R., Strobel, M., Flaxmeier, E., Schuessler, A. "Micro welding for improved radiopacity of nitinol stents." In: M. Mertmann (ed.) *SMST-2004: Proceedings of the International Conference on Shape Memory and Superelastic Technologies.* ASM International, Materials Park. pp. 591-596. 2006.

[12] Scott, H., Ich, O., Yi, Y. "*Stent with attached sleeve marker.*" EP1488763. Endotex Interventional Systems, Inc. 2004.

[13] Siekmeyer, G., Steegmüller, E., Schrader, B., Hegel, A., Strobel, M., Schuessler, A. "Novel micro-joining techniques to improve stent radiopacity. A comparison of welding and riveting processes." In: V. Ramakrishna (ed.) *Medical Device Materials III.* ASM International, Novelty. pp. 57-62. 2006.

[14] Stinson, J. S. "*Medical devices including composites.*" US patent 7641983. Boston Scientific Scimed. 2010.

[15] ASTM Standard F640. "*Standard Test Methods for Determining Radiopacity for Medical Use.*" ASTM International. West Conshohocken, PA. 2012.

[16] European Standard. "*Non active surgical implants. Particular requirements for cardiac and vascular implants. Specific requirements for arterial stents.*" EN 14299:2004. 2004.

[17] ISO 25539:2:2013. "*Cardiovascular implants. Endovascular devices. Part 2: Vascular stents: Balloon dilatation catheters.*" International Organization for Standardization. 2013.

[18] Yunquiang, C., Ti-chiun, C., Michelle, X. Y., Tong, F., Pohl, T., Böhm, S., Durlak, P., Roßmeier, M. "*System and method for multi-image based stent visibility enhancement.*" US8433115 B2. Siemens Corporation. 2013.

[19] Connolley, T., Nash, D., Buffière, J.-Y., Sharif, F., McHugh, P. E. "X-ray micro-tomography of a coronary stent deployed in a model artery." *Medical Engineering & Physics.* 29 (10). pp. 1132-1141. 2007. DOI: 10.1016/j.medengphy.2006.10.016

[20] Colombo, A., Stankovic, G., Moses, J. "Selection of coronary stents." *Journal of the American College of Cardiology.* 40 (6). pp. 1021-1033. 2002. DOI: 10.1016/S0735-1097(02)02123-X

[21] Ring, Gy. "*Pre-clinical evaluation of coronary stents and other endoprotheses.*" Ph.D. dissertation, Department of Materials Science and Engineering. Budapest University of Technology and Economics. 2011.

[22] Ginsztler, J., Major, L., Puskás, Zs., Koós, M., Dobránszky, J., Giese, M., Szabó, B., Albrecht, K. "Development and Manufacturing of Coronary Stents in Hungary." *Material Science Forum.* 537. pp. 631-638. 2007. DOI: 10.4028/www.scientific.net/MSF.537-538.631

[23] Katona, B., Bognár, E., Balázs, B., Nagy, P., Hirschberg, K. "Chemical etching of nitinol stents." *Acta of Bioengineering and Biomechani*cs. 15. pp. 3-8. 2013.